RESEARCH ARTICLE

Phenotypic and Genetic Characterization of Avian Influenza H5N2 Viruses with Intra- and Inter-Duck Variations in Taiwan

Yao-Tsun Li[1], Hui-Ying Ko[1☉], Chang-Chun David Lee[1☉], Ching-Yu Lai[2], Chuan-Liang Kao[1], Chinglai Yang[3], Won-Bo Wang[2]*, Chwan-Chuen King[1]*

1 Institute of Epidemiology and Preventive Medicine, College of Public Health, National Taiwan University (NTU), Taipei, Taiwan, Republic of China (R.O.C), 2 Graduate Institute of Microbiology, College of Medicine, NTU, Taipei, Taiwan, R.O.C, 3 Department of Microbiology and Immunology, Emory University School of Medicine, Atlanta, Georgia, 30322, United States of America

☉ These authors contributed equally to this work.
* wbwang@ntu.edu.tw (WBW); chwanchuen@gmail.com (CCK)

Abstract

Background

Human infections with avian influenza viruses (AIVs) have frequently raised global concerns of emerging, interspecies-transmissible viruses with pandemic potential. Waterfowl, the predominant reservoir of influenza viruses in nature, harbor precursors of different genetic lineages that have contributed to novel pandemic influenza viruses in the past.

Methods

Two duck influenza H5N2 viruses, DV518 and DV413, isolated through virological surveillance at a live-poultry market in Taiwan, showed phylogenetic relatedness but exhibited different replication capabilities in mammalian Madin-Darby Canine Kidney (MDCK) cells. This study characterizes the replication properties of the two duck H5N2 viruses and the determinants involved.

Results

The DV518 virus replicated more efficiently than DV413 in both MDCK and chicken DF1 cells. Interestingly, the infection of MDCK cells by DV518 formed heterogeneous plaques with great differences in size [large (L) and small (S)], and the two viral strains (p518-L and p518-S) obtained from plaque purification exhibited distinguishable replication kinetics in MDCK cells. Nonetheless, both plaque-purified DV518 strains still maintained their growth advantages over the plaque-purified p413 strain. Moreover, three amino acid substitutions in PA (P224S), PB2 (E72D), and M1 (A128T) were identified in intra-duck variations (p518-L vs p518-S), whereas other changes in HA (N170D), NA (I56T), and NP (Y289H) were present in inter-duck variations (DV518 vs DV413). Both p518-L and p518-S strains had the

N170D substitution in HA, which might be related to their greater binding to MDCK cells. Additionally, polymerase activity assays on 293T cells demonstrated the role of vRNP in modulating the replication capability of the duck p518-L viruses in mammalian cells.

Conclusion

These results demonstrate that intra-host phenotypic variation occurs even within an individual duck. In view of recent human infections by low pathogenic AIVs, this study suggests possible determinants involved in the stepwise selection of virus variants from the duck influenza virus population which may facilitate inter-species transmission.

Introduction

Influenza has been a major concern for global health due to dynamic changes through continuous antigenic changes and occasional antigenic shifts resulting from the reassortment of viruses derived from different hosts [1]. Emerging novel influenza viruses, such as the 2006 H5N1 clade 2.2.1 virus in Egypt [2, 3], the 2009 swine-origin pandemic H1N1 virus [4], the 2011–2012 H3N2 variant in the United States [5], the 2013 H7N9 virus from human cases in China [6], and the first reported human H6N1 influenza pneumonia case in Taiwan [7], have highlighted the need for better understanding of the evolution and pathogenicity of avian influenza viruses (AIVs).

Routine virological surveillance in live-poultry markets (LPMs) has become imperative since the outbreaks of H5N1 influenza virus occurred in Hong Kong in 1997 [8]. Most importantly, the information on viral sequences provided clues to the origins of pathogens, and evaluation of inter-species transmission has great value in obtaining these molecular signatures for risk assessment and improved public health preparedness [9, 10]. Moreover, molecular and phenotypic characterizations of AIVs are critical for discovering new mechanisms and determinants involved in virus replication, virus-host interactions, host adaptation and immunopathology [11, 12].

Waterfowl, the major influenza virus reservoir, harbors genes that might contribute to AIVs with the potential to infect humans [12, 13]. Recent findings of H5N1 virus spread among ducks and other avian species suggest that ducks could also play an important role in influenza virus transmission [14, 15]. However, virological studies on dynamic changes in low pathogenic avian influenza (LPAI) viruses in ducks are few. To better monitor AIVs, we initiated a routine virological surveillance of influenza viruses in healthy ducks at a large, wholesale LPM in 2005 [16] and isolated LPAI H5N2 viruses for further characterization [17].

Here we report that the two Taiwan duck influenza H5N2 isolates, DV518 and DV413 [17], with high genetic sequence identities (nucleotides for eight viral genes ranging 99.6–100%) showed differences in their growth efficiencies in both mammalian and avian cells. In addition, heterogeneous viral sub-populations of LPAI viruses with different replication efficiency in the mammalian cells studied did exist within one individual duck influenza DV518 isolate. These findings could help understand the important elements in viral selection, pathogenesis and inter-species transmission from LPAI.

Materials and Methods

Sources of Taiwan duck influenza H5N2 viruses

Several Taiwan duck LAPI H5N2 viruses with different gene constellations that were isolated from fecal droppings in the environment of a live-poultry market of the previous study before

2012 [16] were examined [Surveillance protocol was approved by the Institutional Animal Care and Use Committee (IACUC) at National Taiwan University, Permit Number: 98–10]. Sequence analyses revealed the phylogenetic closeness between the two duck H5N2 viruses—DV518 and DV413 (i.e. parental viruses), with only three amino acid differences in all of the eight gene segments [17]. Therefore, these two virus strains were selected to examine their phenotypic variations in growth properties.

Production of infectious viruses in cell culture

Madin-Darby Canine Kidney epithelial cells (MDCK) and chicken embryo fibroblast cells (DF1) [18] were grown at 37°C in Dulbecco's Modified Eagle Medium (DMEM) (Invitrogen) or Minimum Essential Medium (MEM) (Invitrogen) supplemented with 10% fetal bovine serum (FBS) (Invitrogen), antibiotics and antimycotic reagents containing 100 μg/mL Streptomycin, 100 units/mL Penicillin and 0.25 μg/mL Amphotericin B (Invitrogen), respectively. For viral infection, serum-free media containing 1 or 0.05 μg/mL L-(tosylamido-2-phenyl) ethyl chloromethyl ketone-treated trypsin (TPCK-trypsin) (Thermo) were used during the infection of MDCK and DF1 cells, respectively.

Quantitative RT-PCR to measure viral RNA

Viral RNA (vRNA) was extracted from the supernatant of infected cells by using the QIAamp Viral RNA Mini kit (Qiagen). The standard M-vRNA of influenza virus was transcribed *in vitro* from an M-gene-carrying plasmid, which was constructed as previously described [19]. The tested sample and ten-fold diluted standard of influenza virus M gene RNA (M-vRNA), in which purified RNA concentration was previously measured by spectrophotometer (General Electronic Company), were then reverse-transcribed by SuperScript III (Invitrogen), using Uni-12 primer [20] in parallel.

For quantitation, the tested samples were measured by quantitative RT-PCR for M vRNA. All cDNA samples were subjected to real-time PCR using the KAPA SYBR FAST qPCR kit (KAPA) with AMF (5'-GAGTCTTCTAACCGAGGTCGAAACGTA -3') and FluA-R (5'-CAAAGCGTCTACGCTGCAGTCC-3') primers [19]. Standard curves were constructed by cycle threshold [C_T] values of the diluted M-vRNA standard with known copy numbers.

Plaque assay and plaque-purification of the viruses

The viral stock was first titrated by plaque assay using MDCK cells. Briefly, MDCK cells were seeded on six-well plates and grown until confluent. Ten-fold serial dilutions of the tested samples were performed in duplicate. After one-hour adsorption at 37°C, the inoculum was then removed and a 1:1 mixture of 1% agarose gel and 2X serum-free DMEM with TPCK-trypsin at a final concentration of 2 μg/mL was immediately added as an overlay medium. After 72 hours' incubation at 37°C, the infected cells were fixed with paraformaldehyde and stained with crystal violet. For plaque-purification, approximately 5–10 plaques were picked after 72 hours incubation without fixing the cells and then individually inoculated into SPF eggs. The p518-L and p518-S virus strains were isolated from large and small plaques, respectively through three rounds of plaque purification from the DV518 virus stock, whereas p413 virus was isolated through only one round of plaque purification from the DV413 virus stock for further virological characterization. Experiments for different virus strains were conducted independently to prevent possible cross-contamination. Plaque morphology was examined after each round of plaque purification; and the sizes and numbers of plaques in one well were analyzed by software Image J 1.45A (Wayne Rasband, National Institutes of Health, U.S.A.)

Viral titration by 50% tissue culture infective dose (TCID$_{50}$)

The TCID$_{50}$ method was modified as previously described [21]. The 96-well plates were seeded with 1.5×10^4 MDCK cells per well, and the tested samples were half-log serially diluted by medium containing TPCK-trypsin with at least four repeats. The virus was adsorbed at 37°C for two hours, ending with removal of the inoculum by washing twice. After 72 hours' incubation at 37°C, the culture supernatant was harvested to determine the occurrence of infection by standard hemagglutination assay [22] [i.e. hemagglutination-positive]. Titers were calculated by the Reed-Muench method [23].

Viral sequence analyses

All the studied viruses, from parent stocks to the plaque-purified strains generated during each round of the plaque-purification process, were used for full-genome sequencing. RNA extraction and reverse transcription were performed to obtain cDNA as mentioned above, using the influenza A virus Uni-12 primer [20]. Finally, cDNA was amplified by conventional PCR with a Platinum *Taq* DNA polymerase kit (Invitrogen). All the PCR products were sequenced by the Sanger method and then the sequence data was analyzed, using software of DNAMAN 7 (Lynnon Corp.) or SeqMan in Lasergene package (DNASTAR). Amino acid residues are shown with the H5 numbering system.

Cell binding assay

MDCK and DF1 cells were grown to monolayer in 12-well plates. These two types of cells were then infected with the same copies per cell of the tested viruses, and then incubated at 4°C for one hour. The infected cells were washed with phosphate buffered saline (PBS) to remove unbound virions. Subsequently, Trizol (Invitrogen) was added to extract RNA from infected cells and the RNA was further extracted using the Direct-zol RNA MiniPrep kit (Zymo). The vRNA was quantified by quantitative RT-PCR.

Minigenome assay

Before transfection, human kidney 293T cells were seeded onto 24-well plates and grown until semi-confluent. The cells were then co-transfected with the plasmid pPOL I-Luc-RT, which contains the luciferase open reading frame in negative polarity flanked by the noncoding regions of the NS gene of influenza A/WSN/33 virus [24], and the Renilla-luciferase-expression plasmid pRL-CMV (which serves as a transfection efficiency control) as described [24]. These cells were incubated at 37°C for 24 hours, and then were infected with the tested Taiwan duck H5N2 virus strains at an MOI of 2. The infected cells were harvested at 9 hours post-infection (h p.i.) as described [25], and the luciferase activity was assayed using a dual luciferase assay reagent kit (Promega).

Western blotting

The 293T cells were seeded in six-well plates and grown until semi-confluent. To measure the infection efficiency, cells were infected with the tested p518-L and p518-S strains in serum-free medium without trypsin) at an MOI of 2. At 0.5, 1.5, or 6 h p.i., cell lysates were collected with modified radio-immuno-precipitation assay (RIPA) buffer supplemented with dithio-threitol (DTT) (Sigma) and protease inhibitors (Millipore). Protein content was determined by the Bradford method, using Bio-Rad Protein Assay kit (Bio-Rad). Proteins in these cell lysates were separated by 10% sodium dodecyl sulfate polyacrylamide gel electrophoresis (SDS-PAGE) and transferred to a polyvinylidene fluoride (PVDF) membrane. The membranes

were incubated with rabbit anti-influenza NP antibodies (GeneTex) and mouse anti-Actin antibody (Millipore), and then stained with horseradish peroxidase (HRP)-conjugated secondary antibodies specific for mouse (Jackson) and rabbit (Cell Signaling). The membranes were developed with the enhanced chemiluminescence system (Perkin Elmer), and the images were obtained by the BioSpectrum Imaging System (UVP).

Statistical analysis

Unpaired Student's t-tests were conducted for statistical analyses by using an R program [26].

Nucleotide sequence accession numbers

The nucleotide sequences of the two Taiwan duck H5N2 DV518 and DV413 virus strains obtained in the present study are available from GenBank under accession numbers KP792297-KP792312.

Ethics statement

This research used only cell lines to investigate viral properties. The sources of the three cell lines used in this study, including (1) chicken embryo fibroblast DF1 cells (ATCC CRL-12203), (2) Madin-Darby Canine Kidney epithelial (MDCK) cells (ATCC CCL-34), and (3) human kidney 293T cells (ATCC CRL-3216) were kindly provided by Dr. Ching-Ho Wang, Dr. Chuan-Liang Kao, and Dr. Shiou-Hwei Yeh at the National Taiwan University, respectively. They were all bought from the American Type Culture Collection (ATCC), Rockville, Maryland, USA (http://www.atcc.org). The protocol of surveillance was approved by the Institutional Animal Care and Use Committee (IACUC) at the National Taiwan University [Permit Number: 98–10].

There was no gain of function performed in this study. We also confirm that the funders [National Institutes of Health (NIH) in the USA and the National Science Council [NSC, renamed as the Ministry of Science and Technology (MOST) since March of 2014 in Taiwan, Republic of China] had no role in study design, data collection and analysis, decision to publish or preparation of the manuscript.

Results

### Growth kinetics of the two Taiwan duck H5N2 virus strains in MDCK and DF1 cells

To investigate the replication levels of DV518 and DV413 *in vitro*, we first used quantitative RT-PCR to quantify the vRNAs in both mammalian and avian cell culture supernatants. Fig 1A shows that the MDCK cells infected with DV518 at an MOI of 0.01 generated significantly higher levels of vRNA after 48 h p.i. and 72 h p.i. when compared with those cells infected with DV413 [Mean: $10^{7.03}$ vs $10^{6.54}$ copies/mL (p<0.05) at 48 h p.i. and $10^{6.90}$ vs $10^{6.01}$ copies/mL (p<0.05) at 72 h p.i.]. In addition, chicken DF1 cells infected with these two virus strains at an MOI of 0.1, also showed quite similar results, with DV518 producing a significantly higher level of vRNA at 48 h p.i. than DV413 (Mean: $10^{5.87}$ vs $10^{5.39}$ copies/mL, p<0.05) (Fig 1B).

Besides vRNA levels, infectious virus titers were also quantified by the $TCID_{50}$ method. MDCK cells infected with DV518 at a MOI of 0.1 resulted in significantly higher viral yield at 36 and 48 h p.i. when compared with the same cells infected with DV413. [Mean: DV518 vs DV413: $10^{2.51}$ vs $10^{1.28}$ $TCID_{50}$/mL (p<0.05) at 36 h p.i. and $10^{3.32}$ vs $10^{1.25}$ $TCID_{50}$/mL (p<0.05) at 48 h p.i.] (Fig 1C). Hemagglutination titers also revealed results similar to those of the $TCID_{50}$ method in MDCK cells (Fig 1D). We also used the $TCID_{50}$ and hemagglutination
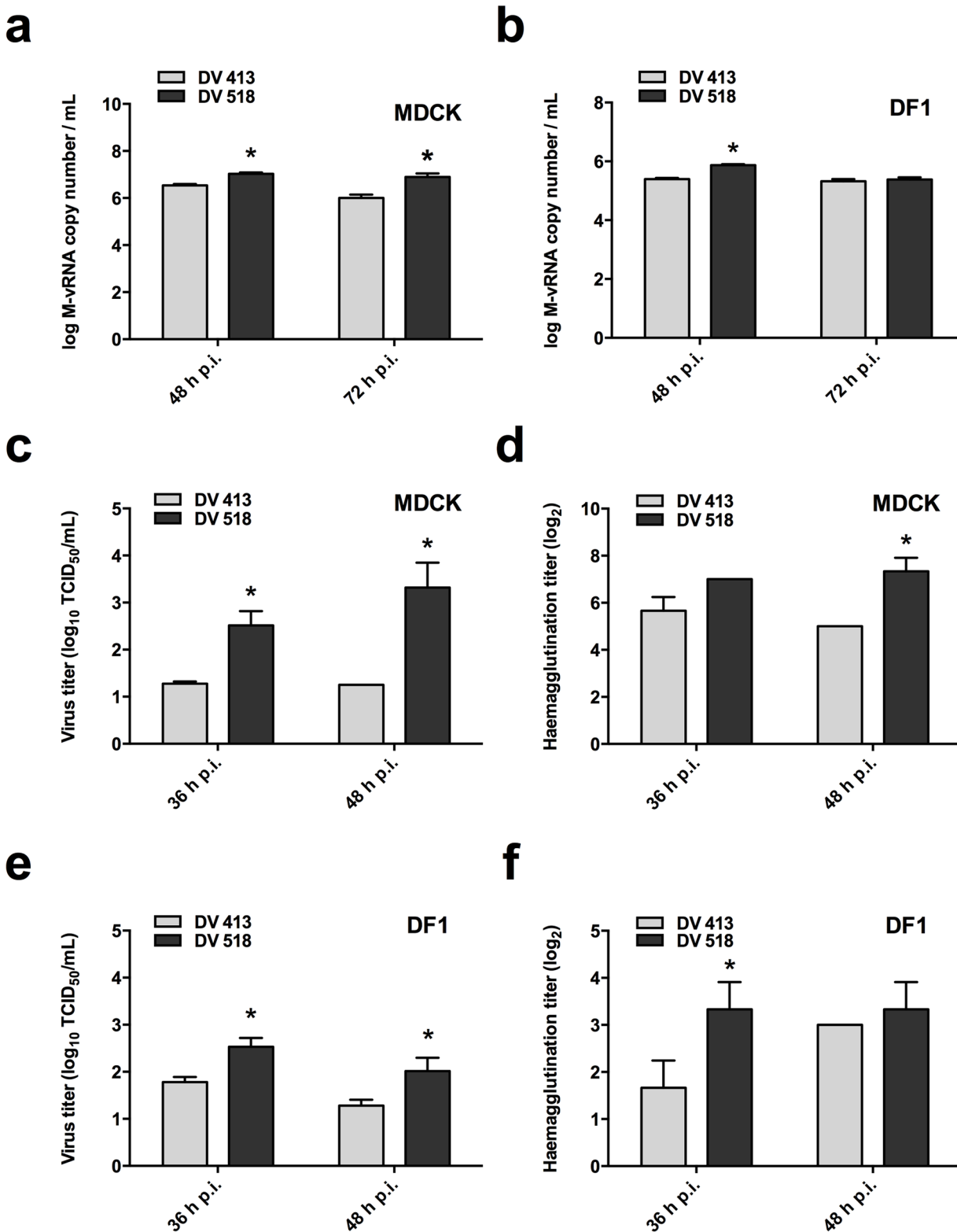
Fig 1. Growth properties of the two Taiwan H5N2 duck viruses in MDCK and DF1 cells. Levels of M-vRNA in the supernatant of (a) MDCK and (b) DF1 cells infected with DV518 and DV413 at MOI of 0.01 and 0.1, respectively, were measured by quantitative RT-PCR. In addition, the viral replication capabilities of DV518 and DV413 in MDCK and DF1 cells at MOI of 0.1 were evaluated by the $TCID_{50}$ method (c and e) and the hemagglutination assay (d and f). Supernatant samples from the infected cells were harvested at the indicated time points. The results are from two independent experiments, presented as means ± standard deviations of triplicate samples. **Abbreviation: MOI**: multiplicity of infection; $\mathbf{TCID_{50}}$: 50% tissue culture infectious dose. *$p < 0.05$

doi:10.1371/journal.pone.0133910.g001
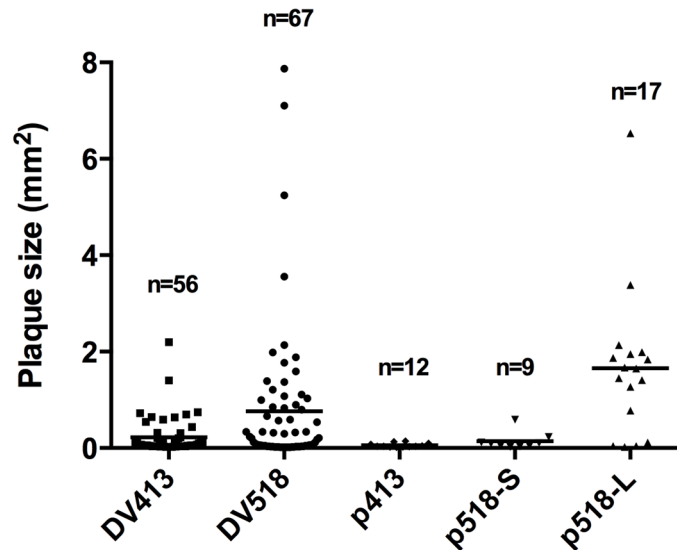
Fig 2. The distributions of plaque sizes in MDCK cells infected with DV518 and DV413 virus strains and the three plaque-purified virus strains. Plaque sizes (mm^2) and numbers of plaques were analyzed by software Image J 1.45A in a representative well infected by DV518 and DV413 virus strains and their plaque-purified strains (p518-L, p518-S, and p413). Mean is shown by a parallel bar, and the total number of plaques is shown at the top, marked as n = 56, 67, 12, 9, and 17, respectively.

doi:10.1371/journal.pone.0133910.g002

methods to quantify virus titers produced in DF1 cells. As shown in Fig 1E and 1F, DV518 produced significantly higher virus titers than DV413 in DF1 cells. Together, these data indicate that DV518 and DV413 differed in their growth in MDCK and DF1 cells, and the DV518 strain produced a higher virus yield.

DV518 virus showed heterogeneous plaque sizes upon infection of MDCK cells

In plaque assays of DV518 and DV413 using MDCK cells, different-sized plaques were observed, implying these duck isolates could be a mixture of heterogeneous viral sub-populations. To test this, we analyzed the distribution of viral plaque sizes of DV518 and DV413 in MDCK cells. The results revealed that the duck DV518 strain generated plaques that were larger and more heterogeneous in size than those generated by the DV413 strain (S1 Fig). Fig 2 shows the distributions of plaque sizes of DV518 and DV413 strains in representative wells. The DV518 strain produced about 25% of the plaques that were larger than 1 mm^2, whereas the DV413 strain had very few plaques larger than 1 mm ($< 3\%$ in Fig 2). In addition, about 25% of both DV518 and DV413 plaques ranged from 0.02 to 0.04 mm^2 in area. These results indicate that the duck DV518 strain was a mixture of heterogeneous viral sub-populations. To further explore this hypothesis, we plaque-purified viruses from large (>1 mm^2) and small plaques in DV518-infected MDCK cells (which were named p518-L and p518-S, respectively) as well as the plaque in DV413-infected MDCK cells (named p413) and then compared their growth properties *in vitro*.

Further analysis of plaque sizes of these purified viral strains (Fig 2 and S1 Fig) showed that the plaques generated by p518-L were larger than those generated by p518-S in MDCK cells (mean area 1.5 mm^2 versus 0.3 mm^2). In addition, the results from the focus-forming assay also verified the above findings (S2 Fig). However, the plaques generated by the p518-S strain were still larger than those plaques (which were pinhead-sized) generated by the p413 strain.

Plaques generated by these purified virus strains were also more homogenous in size, although there was a wider standard deviation (SD) of p518-L, apparently influenced by the outliers (1.35 ± 0.94 mm^2 for p518-L without one outlier, n = 16).

The plaque-purified duck H5N2 p518-L and p518-S virus strains exhibited different growth profiles in MDCK cells

The growth kinetics of these three plaque-purified virus strains (p518-L, p518-S and p413) were simultaneously examined in MDCK and DF1 cells using the hemagglutination method. As shown in Fig 3A, while p518-L produced the highest viral titers, p413-S had the lowest titers in MDCK cells. However, in DF1 cells, these purified viral strains produced comparable, but low, virus titers (Fig 3B). We also used the TCID$_{50}$ method to measure the virus titers produced in MDCK cells. As shown in S3 Fig, p513-L and p513-S showed much higher titers than p413 the titers of which were under the detection limit by using the TCID$_{50}$ method. It should be noted that the TCID$_{50}$ method measures the viruses that can cause a cytopathic effect in MDCK cells. Thus the TCID$_{50}$ method gave much lower titers for those virus strains with weak multiplication efficiency (i.e. p413) than those results obtained from the quantitative RT-PCR and the hemagglutination methods, which measure the amount of virus directly.

To verify the above findings from DF1 cells, we used an *in ovo* system with 14-day-old embryonated SPF eggs to mimic selective pressure for AI viruses in chickens [27, 28]. These three plaque-purified virus strains were inoculated into SPF eggs at 5,000 TCID$_{50}$ units, and the virus yield in allantoic fluid at 48 h p.i. was examined. As shown in Fig 4, p518-L and p518-S grew to titers slightly higher than p413 (the peaking titers of p518-L, p518-S and p413-inoculated eggs were $10^{7.25}$, $10^{6.3}$, and $10^{6.25}$ TCID$_{50}$/mL, respectively), although the differences did not reach statistical significance. This result is consistent with the data shown in Fig 3B. The data also indicate that p413 was able to replicate at low levels in DF1 cells, while it had limited ability to replicate in MDCK cells.
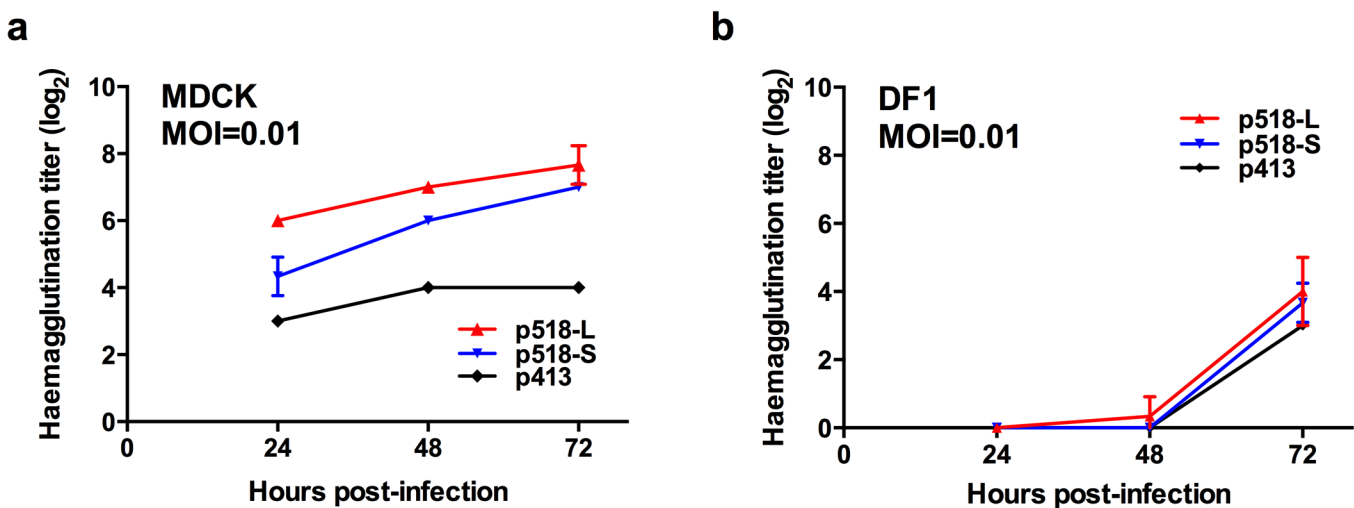
Fig 3. The growth kinetics of the three plaque-purified virus strains (p518-L, p518-S and p413) in MDCK and DF1 cells. MDCK and DF1 cells were infected with p518-L, p518-S, and p413 virus strains at an MOI of 0.01. The supernatants were harvested at the indicated time points. The hemagglutination assays were used to examine the viral growths. The results are shown as means ± standard deviations of triplicate samples. **MOI**: multiplicity of infection

doi:10.1371/journal.pone.0133910.g003
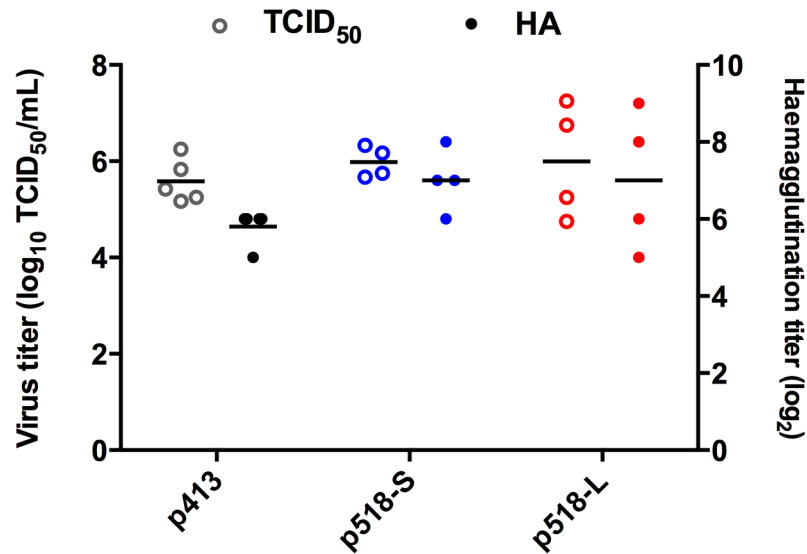
Fig 4. Viral yield in chicken embryonated eggs inoculated with p518-L, p518-S, and p413 virus strains.
Five SPF eggs were inoculated with 4×10^5 TCID$_{50}$ titer of each of the p518-L, p518-S, and p413 virus strains. Eggs were euthanized at 48 h p.i. and their allantoic fluid was collected for measurement of viral load by either TCID$_{50}$ method (empty circles " ") or hemagglutination assay (solid circles "•"). Mean values are shown by parallel bars. Both p518-S and p518-L inoculated groups had one uninfected egg (hemagglutination titer <1), which was excluded from the analyses. **SPF:** Specific pathogen free. **TCID$_{50}$:** 50% tissue culture infectious dose.

doi:10.1371/journal.pone.0133910.g004

Full-genome amino acid sequence analyses of the three plaque-purified H5N2 virus strains (p518-L, p518-S, and p413) and their parental virus strains (DV518 and DV413)

To gain more information on the mechanism involved in phenotypic variations of the plaque-purified virus strains, we sequenced p518-L, p518-S and p413 strains and compared the results with those obtained from the original viral isolates (marked as "original" DV518 and DV413 in Table 1). The original DV518 and DV413 viral stocks were obtained by amplification of the original fecal samples grown in the SPF chicken eggs. Therefore the sequence of DV518 and DV413 most likely represent the sequence of the major viral population in the original fecal samples. Table 1 summarizes the deduced amino acid variations. The purified p518-L and p518-S had the same signature at three amino acid residues (HA[170Asp], NA[56Thr], NP[289His]) as the original DV518 strain. In contrast, both original DV413 and purified p413 strains had different amino acids of HA[170Asn], NA[56Ile], and NP[289Tyr] at these positions (Table 1). In addition, p518-L possessed another two distinct variations in PB2 and M1 proteins (PB2[72Asp], M[182Thr]), compared with the residues at the respective positions shared by both p518-S and p413 strains (PB2[72Glu], M[182Ala]). On the other hand, p518-S had one residue (Pro) in PA at position 224 that was different from p413 and p518-L (PA[Ser224]). It is noteworthy that this PA[224Pro] variation is the only residue where p518-S differed from the original DV518 isolate (PA[Ser224]). Since p518-L and p518-S were obtained by triple plaque purification steps, we also sequenced their original plaques picked up during the first round of purification. The results showed that all molecular signatures described above were also present in the respective original plaques (without double base peaks in the sequence chromatogram), implying that the substitutions we detected did not emerge through selection during the purification procedure (see details in S4 Fig).

Table 1. Amino acid changes detected in eight gene segments of the DV518 and DV413 strains.

Virus	Amino acids at the following positions:					
	PB2	PA	HA	NP	NA	M1
	72	224	170	289	56	182
518-Origin	E	S	**D**	**H**	**T**	A
p518-S	E	**P**	D	H	T	A
P518-L	**D**	S	D	H	T	**T**
413-Origin	E	S	**N**	**Y**	**I**	A
p413	E	S	N	Y	I	A

Sources of information: Data were acquired from viral sequences of the two Taiwan duck H5N2 DV518 and DV413 virus strains in 2006 [17]

Both **518-Origin** and **413-Origin** of Taiwan duck influenza H5N2 viruses represent the viral sequences that were performed directly on the 1st passage of egg culture from the duck fecal droppings that we collected from the floor of a live-poultry market.

p518-L, p518-S: The two virus strains were purified from either large or small "plaques" (with "p" added in the front) after the infection of DV518 in MDCK cells.

Boldface amino acids represent the residue differences between DV518 and DV413 strains and between p518-L and p518-S strains. Residues are shown with H5 numbering system.

doi:10.1371/journal.pone.0133910.t001

The two purified DV518 (p518-L and p518-S) strains showed enhanced binding to MDCK cells

HA proteins, playing a predominant role in receptor binding, influence host range [13], virulence [29], and transmissibility [30, 31] of influenza viruses. Both p518-L and p518-S strains had Asp residue at position 170 (170D) in HA that is different from the 170Asn (170N) in p413. It is possible that the substitution of N170D in HA has the potential to modulate viral binding to the cells. We thus investigated the ability of these viruses to bind to the MDCK and DF1 cells. To perform virus binding assays, MDCK or DF1 cells representing different receptor conformations [32, 33] were incubated with the four duck H5N2 viruses [p518-L, p518-S, p413, or DV30-2 (our earliest duck H5N2 isolate with HA-170Asn)] for comparison. The DV30 virus with a receptor specificity previously characterized by glycoarray as α2,3 preference (Chung-Yi Wu and Chi-Huey Wong, personal communication), the typical avian-type specificity [34, 35], was used to normalize the copy numbers of vRNA binding to the cells. After one hour's incubation at 4°C and extensive wash, the cells were collected for vRNA quantification by quantitative RT-PCR. As shown in Fig 5, both p518-L and p518-S strains had significantly higher capacity to bind to MDCK cells than did p413 virus (p<0.05). In addition, these two p518 strains also had higher capacity to bind to avian DF1 cells than did p413, though the difference among them was insignificant, indicating their common specificity to α2,3 receptors. All these results suggest that the substitution of N170D in HA may have the potential to modulate viral binding to MDCK cells, contributing to the better growth of DV518 and its derived two plaque-purified strains in mammalian cells.

The p518-L virus strain showed higher polymerase activity in 293T cells

The p518-L and p518-S strains differed in three amino acids in three proteins of PB2, PA and M1. PB2 and PA are the components of viral polymerase that functions in viral transcription and replication [12]. We thus investigated whether p518-L and p518-S exhibited different polymerase activity in mammalian 293T cells. To assess possible differences in viral polymerase activity of these two p518 strains, a polymerase reporter plasmid and a Renilla-luciferase- expression
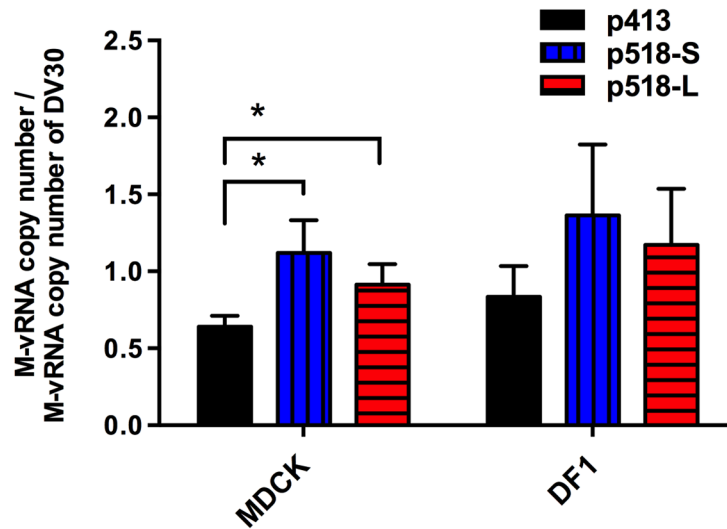
Fig 5. Cell binding ability of p518-L, p518-S and p413 virus strains to MDCK and DF1 cells. MDCK and DF1 cell monolayers were infected with p518-L, p518-S and p413 viruses at the same copy number and incubated at 4°C for 1 h. After extensive wash, viral RNAs were extracted from the infected cells and influenza viral M RNAs were quantified by quantitative RT-PCR. The copy numbers of M RNA attached to the cells were normalized to that of DV30 in each set of data. Results are shown as means with standard deviations in three experiments. ***p<0.05. RT-PCR:** Reverse transcription-polymerase chain reaction.

doi:10.1371/journal.pone.0133910.g005

plasmid (which serves as a transfection efficiency control) were co-transfected into 293T cells. These cells were then infected with either p518-L or p518-S virus, and the luciferase activity was evaluated at 9 h p.i. As shown in Fig 6, p518-L exhibited significantly higher luciferase activity than p518-S in 293T cells, suggesting that the former virus had higher polymerase activity than the latter virus.

To determine whether the difference in luciferase activity observed in Fig 6 is due to the difference in viral entry efficiency, we assessed the viral entry of p518-L and p518-S by examining the abundance of NP protein at early time points after infection. As shown in Fig 7, the abundance of NP protein at early time points (0.5 and 1.5 h p.i.) was lower in p518-L infected 293T cells than in p518-S infected 293T cells; importantly, comparable NP protein levels were detected in cells infected by these two strains at 6 h p.i. Therefore, the higher luciferase activity observed in 518-L-infected 293T cells is indeed due to its greater polymerase activity but not due to its entry efficacy.

Discussion

Poultry ducks carrying LPAI viruses have played critical roles in virus evolution [14, 15], including the novel H5N1 viruses found in Hong Kong that have impacted human health since 1997 [11]. However, few viral replication studies focus on duck LPAI H5N2 viruses. In this study, we characterized the phenotypic variations between the two genetically close duck LPAI H5N2 influenza viruses and revealed three major findings that helped us better understand the epidemiological aspects of influenza. First, variations of LPAI H5N2 viruses involved both intra-host and inter-host levels in ducks that may increase viral diversity, population dynamics, and continuous evolution. Second, intra-duck variations (shown in p518-L vs p518-S) included three residue substitutions in PA (P224S), PB2 (E72D), and M1 (A128T), whereas inter-duck variations (shown in DV518 vs DV413) contained the other three mutations in HA (N170D), NA (I56T), and NP (Y289H). These differences indicate that two levels of viral variations were
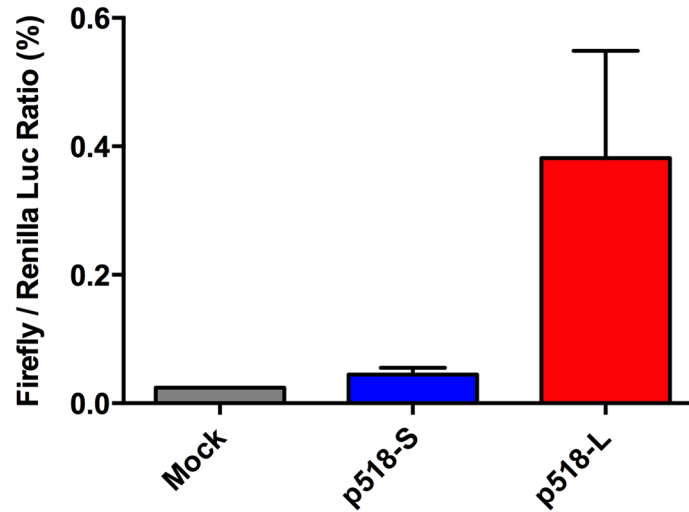
Fig 6. The viral polymerase activity of p518-S and p518-L strains in MDCK cells measured by minigenome assays. The viral polymerase activity of p518-S and p518-L strains was measured by minigenome assays as described in Materials and Methods. Data are presented as the ratios of firefly luciferase signal to Renilla luciferase signal, with means and standard deviations in triplicate experiments.

doi:10.1371/journal.pone.0133910.g006

involved in the mutations of different genes. Third, phenotypic variations of duck influenza p518-L strain with better replication in MDCK cells (compared to p518-S and p413) imply that duck-LPAI viruses may have a stronger potential to infect mammalian hosts under certain epidemiological settings [30, 36, 37]. Taken together, these findings provide new insight on the genotypic and phenotypic variations of LPAI H5N2 viruses from an individual duck to the entire duck population, prior to the process of expanding epizootic potential, and infecting other hosts.

Identifying the molecular determinants involved in genotypic and phenotypic variations of duck influenza viruses can help to understand mechanisms for viral persistence in nature, inter-species transmission, and elevated pathogenicity and virulence leading to severe
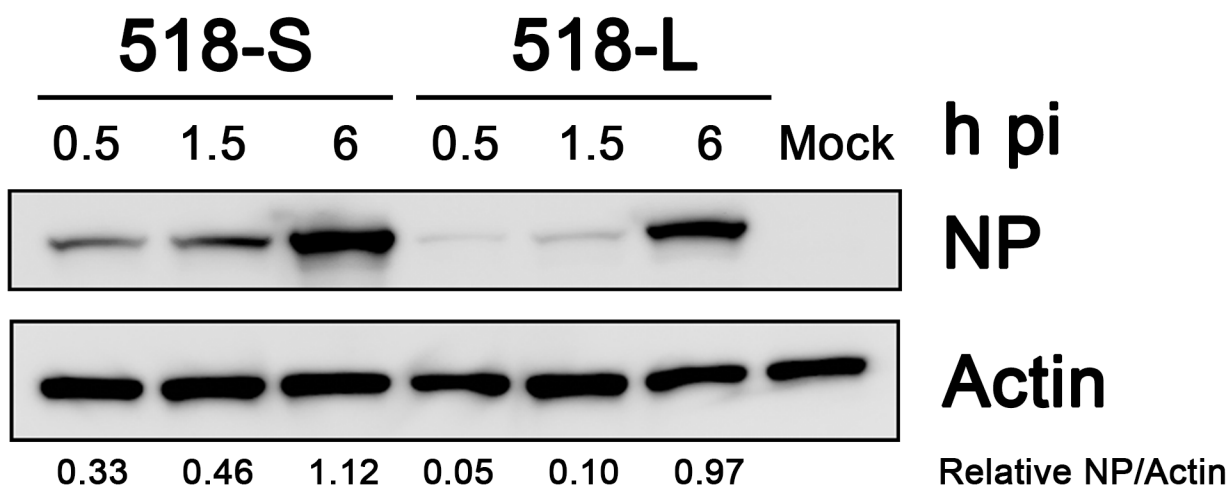
Fig 7. Evaluation of viral entry efficiency for p518-S and p518-L virus strains in 293T cells. The 293T cells were infected with p518-S and p518-L viruses at an MOI of 2. Cell lysates were collected at 0.5, 1.5 and 6 h p.i. and were examined by Western blot using anti-NP and anti-actin antibodies. Levels of protein and relative ratios of NP/Actin were analyzed by software Image J. **MOI**: multiplicity of infection

doi:10.1371/journal.pone.0133910.g007

epidemics and pandemics [13]. AIVs in waterfowl (predominantly wild ducks), which are important viral maintenance hosts, vary in infection susceptibility, exit routes, levels of viral excretion, and shedding patterns among different wild duck species [38]. Generally, these natural hosts infected with AIVs are asymptomatic or have mild infections. Several species of wild and domestic ducks are "silent spreaders" serving as the "Trojan horses" for influenza viruses [39]. Most importantly, certain AIV strains have the capability to cross host range barriers and infect other species, including humans. However, the selection mechanisms of LPAI virus among poultry ducks, which bridge natural maintenance hosts and other host species, are not well understood. Our data showed that the duck DV518 strain can grow to titers significantly higher than the duck DV413 strain in both mammalian MDCK and avian DF1 cell lines, thus implying the existence of factors that may contribute to viral replication. Moreover, the three plaque-purified strains, p518-L, p518-S, and p413, exhibited more complicated replication profiles: p518-L and p518-S replicated more efficiently than p413 in MDCK cells but showed comparable efficiency to that of p413 in DF1 cells. Evaluations of viral cell binding were in accordance with the growth advantages of both p518-L and p518-S strains in MDCK cells. Furthermore, varied viral polymerase activities between these two strains in 293T cells suggest that the difference in viral replication may be conferred by polymerase activities in host-specific cell lines. These findings not only support the importance of routine virological surveillance to understand and identify the phenotypic diversity of duck influenza viruses isolated from the same and different ducks, but also provide important information about virus evolution in both individual and population levels.

For intra-host variants, p518-L showed significantly higher polymerase activity in 293T cells when compared to p518-S. Detailed sequence analysis indicated that these two variants differed only at three positions (Table 1), and two of them are located in the components of the viral polymerase complex. These data indicate that the replication advantage of the AIV variants with minor genetic variation can be selected for within the same duck. How the amino acid variations in PB2, PA, and M1 contribute to the higher polymerase activity in p513-L is unclear. The minigenome assay was conducted at 9 h p.i. (a single replication cycle). This would exclude the possible involvement of mutation in M1, a protein known to play a role in vRNP export [40]. Position 72 in the PB2 is located in the PB2-N1 subdomain buttressing the PB1 thumb domain [41]. However, it is less likely that the mutation (from glutamate to aspartate without changing the charge) in p513-L would affect the function of the PB2 protein significantly. In PA, the mutation of S224P with other amino acid substitutions has been shown to increase the replication of duck H5N1 viruses in duck primary embryo fibroblast cells [42], and elevate viral virulence in a mouse model [42]. Whether the change at position 224 in PA (from proline to serine) may increase the polymerase activity of p513-L virus requires further investigation.

By contrast, inter-host variations of the two Taiwan-H5N2 DV518 and DV413 viruses were isolated from fecal droppings between poultry ducks (collected on July 28 and September 7, 2006 at a wholesale LPM (16) where ducks came from Yilan and Yunlin counties). These two viruses involved another three amino acid changes (N170D, I56T, and Y289H) in HA, NA, and NP, respectively [43–45]. DV518, p518-L and p518-S strains all have a 170D residue in HA in contrast to a 170N in DV413 and p413. Our data indicated that p518-L and p518-S viruses bind to MDCK cells, which possess both α2,6 and α2,3 receptors [33], more efficiently than the p413 virus (Fig 5). Furthermore, these three virus strains showed no significant difference in binding to A549 and DF1 cells (S5 Fig), which possess predominantly α2,6 and α2,3 receptors, respectively [32, 33], indicating that the receptor specificity of these viruses may not have been altered. Position 170 (or 158 in H3 structural numbering) is located at the tip of the HA (S6 Fig), near the receptor binding domain (RBD) in the globular head of HA1 [46]. This

N170D (or N158D) mutation in HA has been correlated with better aerosol transmissibility of H5N1 viruses in ferrets [31] and guinea pigs [47] as well as human H5N1 cases in Vietnam and Egypt [48, 49]. Moreover, a quail-adapted duck H3N2 virus (i.e. virus adaption in **terrestrial birds** from aquatic birds) possessing HA-170D mutation replicated more efficiently in MDCK cells, even though these viruses had receptor specificities similar to those of the parental duck virus, and exhibited the potential to infect human cells *in vitro* and *ex vivo* [36]. The possible mechanism of this selection advantage might be attributable to the role of aspartate in increasing the negative charge on the surface of HA (a marker for adaptation to cultured mammalian cells) [50] (S6A and S6B Fig illustrate the polarity change of HA). Taken together, these results and findings by others suggest that N170D of HA does not alter the receptor specificity but may enhance its receptor-binding affinity by forming a more stable structure [31, 50, 51]. In other words, both p513-L and p513-S show enhanced binding to MDCK cells and the substitution of N170D in HA has the potential to modulate viral binding to MDCK cells. Whether the N170D mutation does contribute to the better binding of p518-L and p518-S to MDCK cells requires further investigation by using reverse genetics methods.

NA is the sialidase on a viral membrane [52], known to be associated with virion release and dissemination [53, 54]. It has been shown recently that NA can modulate receptor binding [55, 56]. However, position 56 in NA is located in the stalk region of the glycoprotein embedded in the membrane, not in the enzymatically active region interacting with sialyglycans [52, 57]. It is less likely that I56T mutation in NA would influence the binding of p513-L and p513-S to MDCK cells. NP protein is involved in resistance to the interferon-induced antiviral factor, Mx [58, 59] and cellular immunity [60, 61]. Several mutations in NP, including Y289H (located in the region predicted to interact with PB2 at the NP-NP interaction site) [62, 63], were recently identified in adaptation of the novel 2009 H1N1 virus to humans [64, 65]. These NP mutations also allow the H5N1 virus to escape from human MxA by inhibiting the host innate immune response to Mx1 [65]. DV518, p518-L and p518-S possess the 289H in NP. This may make them become more resistant to the host's antiviral strategies. Whether HA (N170D), NA (I56T), and NP (Y289H) mutations alone or in combination contribute to the growth advantage of DV518, p518-L, and p513-S in MDCK cells requires further investigation by using reverse genetics method.

The evolution of influenza viruses is a continuous process of interactions between viruses and hosts. Due to the infidelity of viral RNA-dependent RNA polymerase and large population sizes, many different genetic alterations may occur during RNA genome replication. Among these heterogeneous viral populations, minor viral variants may have significant implications for quasispecies evolution [66]. Our duck LPAI H5N2 viruses had slow evolution and stable viral sequences, because the viral sequences remained the same after one passage in chicken eggs and through several steps of plaque-purification (data not shown). However, the selection of AIVs does occur in poultry ducks, because neither p518-L nor p518-S is identical to the original DV518 isolate in full-genome sequences. This result indicates that the overall virus population derived from the field is a mixture of heterogeneous sub-populations of viral variants. Our finding on intra- and inter-duck phenotypic variations of the viruses which occurred at a cellular level is consistent with previous studies from duck samples demonstrating varied biological characteristics [14] and LPAI H1N9 and H6N1 isolates from wild birds replicates in ferrets [67]. For inter-duck variants, DV518 had growth advantage over DV413. For intra-duck variants, a minor sub-population of variants such as p518-L may have growth advantage in mammalian cells, causing health problem in humans after further evolution.

There are four major limitations to this study. First, the viral mutations identified from this study need further investigation, using reverse genetic approaches to determine whether a single mutation or multiple co-mutations were required to enhance viral replication in

mammalian cells. Moreover, whether DV518 and its derivative viruses could multiply more efficiently than DV413 and its derivative virus in mice or other primates needs to be investigated. Second, the original samples amplified in the SPF eggs may not represent the viral population in the host [17]. Third, the two genetically close duck H5N2 viruses we studied cannot reflect the whole of viral population dynamics and selection in ducks, nor the previously reported H5N2 viruses in chickens in Taiwan [13]. In reality, whether the studied duck viruses have other additional unidentified subpopulations remains unclear. Fourth, the roles of host or environmental factors or concurrent infection of multiple subtypes of AIVs in intra- or inter-host evolution of duck H5N2 viruses deserve further investigation. Fully understanding the spectrum of viral variants (various percentages of the subvariants) and their roles in viral phenotypic variations through selection and fitness with trends in becoming dominant subvariants requires more modernized laboratory methods (such as reverse genetics, next generation sequencing) to provide stronger conclusion.

In summary, this study reveals several molecular determinants that may enhance cell binding and replication of duck LPAI H5N2 virus in MDCK cells. As anti-H5N2 seropositive poultry workers were detected [68], molecular markers for increasing viral replication as well as higher ability to inhibit antiviral immunity will be helpful in selecting the best strain for a future cell-based human H5N2 vaccine. The higher binding to and the greater replication capability of DV-518 (particularly DV-518-L) in MDCK cells implies that duck influenza virus sub-variants may possess potential for inter-species transmission to mammalian hosts. Such mutation events involve a series of host adaptations and selection, which may result in a novel virus with increasing replication efficiency, pathogenicity, and pandemic potential, as recently observed with novel H5N8 AIVs causing poultry outbreaks worldwide [69, 70]. Taken together, the integrated information from the micro-evolution of the virus to population dynamics can provide us with better clues about various selection mechanisms involving route of infection, receptor binding, replication efficiency, virion packaging, herd immunity, and efficient transmissibility [71]. In view of the most recent severe and fatal human cases caused by novel LPAI H7N9, H6N1 and H10N8 viruses [6, 7, 72], there is an increasing need to gain more knowledge about molecular determinants associated with host range and inter-species transmission of LPAI viruses. Therefore, efforts to establish integrated surveillance in areas involving wild birds, poultry ducks, chickens and mammalian hosts are urgently needed. By using whole-genome, deep pyrosequencing analysis and phenotypic characterizations, the evolutionary features of AIVs at a sub-population level after passaging through either avian or mammalian cells can be used to identify host-specific molecular markers associated with alterations in viral replication [61, 73]. A series of studies focused on an H7N9 drug-resistant subpopulation and their fitness *in vivo* can serve as a good example [74, 75]. This effort will help us fully understand the selection mechanisms and dynamic changes of molecular determinants in different host species at both micro- and macro-levels, leading to improved risk assessment, vaccine development and pandemic preparedness.

Supporting Information

S1 Fig. Plaque morphologies of DV518, DV413 and their plaque-purified strains (p518-S, p518-L, p413) on MDCK cells. MDCK cells were infected with DV413, DV518, p413, p518-S and p518-L virus strains. After incubation at 37°C for 72 h, cells were fixed by paraformaldehyde and stained with crystal violet. Mean plaque area (mm^2) of plaque in a representative well for each strain was analyzed by software Image J, and was shown as mean ± standard deviations in the parentheses.
(PDF)

S2 Fig. Plaque morphologies of p518-L and p518-S viruses shown by focus- forming assay on MDCK cells. MDCK cells were infected with p518-L or p518-S viruses. After incubation at 37°C for 48 h, infected cells were treated with a mixture of mouse anti-influenza M monoclonal antibody (Millipore) and mouse anti-influenza NS1 monoclonal antibody (Santa Cruz Biotechnology) after fixation. The HRP-conjugated anti-mouse secondary antibody (Jackson) was then added and the foci were subsequently developed by adding peroxidase substrate using a commercial kit (Vector Laboratories).
(PDF)

S3 Fig. The growth kinetics of the three plaque-purified virus strains (p518-L, p518-S and p413) in MDCK cells as determined by $TCID_{50}$ method. MDCK cells were infected with p518-L, p518-S, and p413 virus strains at an MOI of 0.01. The supernatants were harvested at the indicated time points. The $TCID_{50}$ method was used to examine the viral growths. The results are shown as means ± standard deviations of triplicate samples.
(PDF)

S4 Fig. Chromatogram comparing nucleotide sequences of HA, PA and NP in parental viruses (DV518 and DV413) and a series of plaque-purified viruses. Abbreviations: 518, DV518 virus; 413, DV413 virus; S-P1, S-P2, and S-P3, small-plaque virus obtained by the first, second, and third round of plaque purification of DV518, respectively; L-P1, L-P2, and L-P3, large-plaque virus obtained by the first, second, and third round of plaque purification of DV518, respectively; 413-P1, virus obtained by first-round plaque purification of DV413.
(PDF)

S5 Fig. p518-L, p518-S and p413 virus strains showed no difference in binding to A549 and DF1 cells. A549 and DF1 cell monolayers were infected with p518-L, p518-S and p413 viruses at the same copy number and then incubated at 4°C for 1 h. After extensive wash, viral RNAs were extracted from the infected cells and influenza viral M RNAs were quantified by quantitative RT-PCR. The copy numbers of M RNA attached to the cells were normalized to that of DV30 in each set of data. Results are shown as means with standard deviations in three experiments.
(PDF)

S6 Fig. Modeled surface polarities and position 170 in HA protein. Surface polarities of HA with positions of 170D (a) and 170N (b) are shown. Position 170 (or 158 in H3 numbering) of HA is at the top of the HA molecule (c). The orange region, HA 161–175, represents the residues changed to the amino acids possessed by DV518 or DV413 (d). All structures shown are based on the backbone of A/Viet Nam/1203 (pdb: 2FK0).
(PDF)

Acknowledgments

Author Contributions

Conceived and designed the experiments: CCK WBW. Performed the experiments: YTL HYK CCL CYL. Analyzed the data: YTL HYK CCL. Contributed reagents/materials/analysis tools: CLK WBW. Wrote the paper: YTL CCK WBW. Paper review and discussion: CY.

References

1. Medina RA, Garcia-Sastre A. Influenza A viruses: new research developments. Nat Rev Microbiol. 2011; 9(8):590–603. doi: 10.1038/nrmicro2613 PMID: 21747392.

2. WHO. Cumulative number of confirmed human cases of avian influenza A(H5N1) reported to WHO. Available from: http://www.who.int/influenza/human_animal_interface/H5N1_cumulative_table_archives/en/.

3. Webster RG, Govorkova EA. H5N1 influenza—continuing evolution and spread. N Engl J Med. 2006; 355(21):2174–7. doi: 10.1056/NEJMp068205 PMID: 17124014.

4. Novel Swine-Origin Influenza A Virus Investigation Team, Dawood FS, Jain S, Finelli L, Shaw MW, Lindstrom S, et al. Emergence of a novel swine-origin influenza A (H1N1) virus in humans. N Engl J Med. 2009; 360(25):2605–15. doi: 10.1056/NEJMoa0903810 PMID: 19423869.

5. Wong KK, Greenbaum A, Moll ME, Lando J, Moore EL, Ganatra R, et al. Outbreak of influenza A (H3N2) variant virus infection among attendees of an agricultural fair, Pennsylvania, USA, 2011. Emerg Infect Dis. 2012; 18(12):1937–44. doi: 10.3201/eid1812.121097 PMID: 23171635; PubMed Central PMCID: PMC3557885.

6. Lee SS, Wong NS, Leung CC. Exposure to avian influenza H7N9 in farms and wet markets. Lancet. 2013; 381(9880):1815. doi: 10.1016/S0140-6736(13)60949-6 PMID: 23664058.

7. Wei SH, Yang JR, Wu HS, Chang MC, Lin JS, Lin CY, et al. Human infection with avian influenza A H6N1 virus: an epidemiological analysis. The Lancet Respiratory medicine. 2013; 1(10):771–8. doi: 10.1016/S2213-2600(13)70221-2 PMID: 24461756.

8. Webster RG. Wet markets—a continuing source of severe acute respiratory syndrome and influenza? Lancet. 2004; 363(9404):234–6. doi: 10.1016/S0140-6736(03)15329-9 PMID: 14738798.

9. Subbarao K, Klimov A, Katz J, Regnery H, Lim W, Hall H, et al. Characterization of an avian influenza A (H5N1) virus isolated from a child with a fatal respiratory illness. Science. 1998; 279(5349):393–6. PMID: 9430591.

10. Hatta M, Gao P, Halfmann P, Kawaoka Y. Molecular basis for high virulence of Hong Kong H5N1 influenza A viruses. Science. 2001; 293(5536):1840–2. doi: 10.1126/science.1062882 PMID: 11546875.

11. Guan Y, Shortridge KF, Krauss S, Webster RG. Molecular characterization of H9N2 influenza viruses: were they the donors of the "internal" genes of H5N1 viruses in Hong Kong? Proc Natl Acad Sci U S A. 1999; 96(16):9363–7. PMID: 10430948; PubMed Central PMCID: PMC17788.

12. Webster RG, Bean WJ, Gorman OT, Chambers TM, Kawaoka Y. Evolution and ecology of influenza A viruses. Microbiol Rev. 1992; 56(1):152–79. PMID: 1579108; PubMed Central PMCID: PMC372859.

13. Horimoto T, Kawaoka Y. Pandemic threat posed by avian influenza A viruses. Clin Microbiol Rev. 2001; 14(1):129–49. doi: 10.1128/CMR.14.1.129–149.2001 PMID: 11148006; PubMed Central PMCID: PMC88966.

14. Hulse-Post DJ, Sturm-Ramirez KM, Humberd J, Seiler P, Govorkova EA, Krauss S, et al. Role of domestic ducks in the propagation and biological evolution of highly pathogenic H5N1 influenza viruses in Asia. Proc Natl Acad Sci U S A. 2005; 102(30):10682–7. doi: 10.1073/pnas.0504662102 PMID: 16030144; PubMed Central PMCID: PMC1180796.

15. Li KS, Guan Y, Wang J, Smith GJ, Xu KM, Duan L, et al. Genesis of a highly pathogenic and potentially pandemic H5N1 influenza virus in eastern Asia. Nature. 2004; 430(6996):209–13. doi: 10.1038/nature02746 PMID: 15241415.

16. Lin H-P. Virological and serological surveillance of avian influenza viruses in live-bird markets and poultry-related workers in Taiwan and Kinmen during 2005–2007 (Master thesis): National Taiwan University Library (http://www.lib.ntu.edu.tw/en); 2007.

17. Lee C-C. Molecular Epidemiology of Avian Influenza Viruses in A Live Bird Market in Taiwan during 2005–2006 (Master thesis): National Taiwan University Library (http://www.lib.ntu.edu.tw/en); 2008.

18. Himly M, Foster DN, Bottoli I, Iacovoni JS, Vogt PK. The DF-1 chicken fibroblast cell line: transformation induced by diverse oncogenes and cell death resulting from infection by avian leukosis viruses. Virology. 1998; 248(2):295–304. doi: 10.1006/viro.1998.9290 PMID: 9721238.

19. Kao CL, Chan TC, Tsai CH, Chu KY, Chuang SF, Lee CC, et al. Emerged HA and NA mutants of the pandemic influenza H1N1 viruses with increasing epidemiological significance in Taipei and Kaohsiung, Taiwan, 2009–10. PLoS One. 2012; 7(2):e31162. doi: 10.1371/journal.pone.0031162 PMID: 22328930; PubMed Central PMCID: PMC3273476.

20. Hoffmann E, Stech J, Guan Y, Webster RG, Perez DR. Universal primer set for the full-length amplification of all influenza A viruses. Arch Virol. 2001; 146(12):2275–89. PMID: 11811679.

21. Szretter KJ, Balish AL, Katz JM. Influenza: propagation, quantification, and storage. Current protocols in microbiology. 2006;Chapter 15:Unit 15G 1. doi: 10.1002/0471729256.mc15g01s3 PMID: 18770580.

22. Webster RG, Cox N, Stohr K. WHO manual on animal influenza diagnosis and surveillance: World Health Organization, Department of Communicable Disease Surveillance and Response; 2002.

23. Reed LJ, Muench H. A simple method of estimating fifty per cent endpoints. Am J Epidemiol. 1938; 27 (3):493–7.

24. Hsu WB, Shih JL, Shih JR, Du JL, Teng SC, Huang LM, et al. Cellular protein HAX1 interacts with the influenza A virus PA polymerase subunit and impedes its nuclear translocation. J Virol. 2013; 87 (1):110–23. doi: 10.1128/JVI.00939-12 PMID: 23055567; PubMed Central PMCID: PMC3536397.

25. Lang V, Marjuki H, Krauss SL, Webby RJ, Webster RG. Different incubation temperatures affect viral polymerase activity and yields of low-pathogenic avian influenza viruses in embryonated chicken eggs. Arch Virol. 2011; 156(6):987–94. doi: 10.1007/s00705-011-0933-z PMID: 21302122; PubMed Central PMCID: PMC3551446.

26. R. The R Project for Statistical Computing. Available from: http://www.r-project.org.

27. Horimoto T, Kawaoka Y. Molecular changes in virulent mutants arising from avirulent avian influenza viruses during replication in 14-day-old embryonated eggs. Virology. 1995; 206(1):755–9. PMID: 7831837.

28. Horimoto T, Kawaoka Y. A possible mechanism for selection of virulent avian influenza A viruses in 14-day-old embryonated eggs. J Vet Med Sci. 1998; 60(2):273–5. PMID: 9524959.

29. Yamada S, Suzuki Y, Suzuki T, Le MQ, Nidom CA, Sakai-Tagawa Y, et al. Haemagglutinin mutations responsible for the binding of H5N1 influenza A viruses to human-type receptors. Nature. 2006; 444 (7117):378–82. doi: 10.1038/nature05264 PMID: 17108965.

30. Yen HL, Liang CH, Wu CY, Forrest HL, Ferguson A, Choy KT, et al. Hemagglutinin-neuraminidase balance confers respiratory-droplet transmissibility of the pandemic H1N1 influenza virus in ferrets. Proc Natl Acad Sci U S A. 2011; 108(34):14264–9. doi: 10.1073/pnas.1111000108 PMID: 21825167; PubMed Central PMCID: PMC3161546.

31. Imai M, Watanabe T, Hatta M, Das SC, Ozawa M, Shinya K, et al. Experimental adaptation of an influenza H5 HA confers respiratory droplet transmission to a reassortant H5 HA/H1N1 virus in ferrets. Nature. 2012; 486(7403):420–8. doi: 10.1038/nature10831 PMID: 22722205; PubMed Central PMCID: PMC3388103.

32. Kumari K, Gulati S, Smith DF, Gulati U, Cummings RD, Air GM. Receptor binding specificity of recent human H3N2 influenza viruses. Virol J. 2007; 4:42. doi: 10.1186/1743-422X-4-42 PMID: 17490484; PubMed Central PMCID: PMC1876801.

33. Lee CW, Jung K, Jadhao SJ, Suarez DL. Evaluation of chicken-origin (DF-1) and quail-origin (QT-6) fibroblast cell lines for replication of avian influenza viruses. J Virol Methods. 2008; 153(1):22–8. doi: 10.1016/j.jviromet.2008.06.019 PMID: WOS:000259340200004.

34. Connor RJ, Kawaoka Y, Webster RG, Paulson JC. Receptor specificity in human, avian, and equine H2 and H3 influenza virus isolates. Virology. 1994; 205(1):17–23. doi: 10.1006/viro.1994.1615 PMID: 7975212.

35. Nicholls JM, Chan RW, Russell RJ, Air GM, Peiris JS. Evolving complexities of influenza virus and its receptors. Trends Microbiol. 2008; 16(4):149–57. doi: 10.1016/j.tim.2008.01.008 PMID: 18375125.

36. Yamada S, Shinya K, Takada A, Ito T, Suzuki T, Suzuki Y, et al. Adaptation of a duck influenza A virus in quail. J Virol. 2012; 86(3):1411–20. doi: 10.1128/JVI.06100-11 PMID: 22090115; PubMed Central PMCID: PMC3264366.

37. Subbarao EK, London W, Murphy BR. A single amino acid in the PB2 gene of influenza A virus is a determinant of host range. J Virol. 1993; 67(4):1761–4. PMID: 8445709; PubMed Central PMCID: PMC240216.

38. Costa TP, Brown JD, Howerth EW, Stallknecht DE. Variation in viral shedding patterns between different wild bird species infected experimentally with low-pathogenicity avian influenza viruses that originated from wild birds. Avian Pathol. 2011; 40(2):119–24. doi: 10.1080/03079457.2010.540002 PMID: 21500030.

39. Kim JK, Negovetich NJ, Forrest HL, Webster RG. Ducks: the "Trojan horses" of H5N1 influenza. Influenza Other Respir Viruses. 2009; 3(4):121–8. doi: 10.1111/j.1750-2659.2009.00084.x PMID: 19627369; PubMed Central PMCID: PMC2749972.

40. Martin K, Helenius A. Nuclear transport of influenza virus ribonucleoproteins: the viral matrix protein (M1) promotes export and inhibits import. Cell. 1991; 67(1):117–30. PMID: 1913813.

41. Pflug A, Guilligay D, Reich S, Cusack S. Structure of influenza A polymerase bound to the viral RNA promoter. Nature. 2014; 516(7531):355–60. doi: 10.1038/nature14008 PMID: 25409142.

42. Song J, Feng H, Xu J, Zhao D, Shi J, Li Y, et al. The PA protein directly contributes to the virulence of H5N1 avian influenza viruses in domestic ducks. J Virol. 2011; 85(5):2180–8. doi: 10.1128/JVI.01975-10 PMID: 21177821; PubMed Central PMCID: PMC3067757.

43. Lim KL, Jazayeri SD, Yeap SK, Mohamed Alitheen NB, Bejo MH, Ideris A, et al. Antibody and T cell responses induced in chickens immunized with avian influenza virus N1 and NP DNA vaccine with chicken IL-15 and IL-18. Res Vet Sci. 2013; 95(3):1224–34. doi: 10.1016/j.rvsc.2013.07.013 PMID: 23948357.

44. Ashour J, Schmidt F, Hanke L, Cragnolini J, Cavallari M, Altenburg A, et al. Intracellular expression of camelid single domain antibodies specific for influenza virus nucleoprotein (NP) uncovers distinct features of its nuclear localization. J Virol. 2014. doi: 10.1128/JVI.02693-14 PMID: 25540369.

45. Russell RJ, Gamblin SJ, Skehel JJ. Influenza glycoproteins: Hemagglutinin and neuraminidase. Textbook of Influenza, 2nd Edition. 2013:67–100.

46. Stevens J, Blixt O, Tumpey TM, Taubenberger JK, Paulson JC, Wilson IA. Structure and receptor specificity of the hemagglutinin from an H5N1 influenza virus. Science. 2006; 312(5772):404–10. doi: 10.1126/science.1124513 PMID: 16543414.

47. Zhang Y, Zhang Q, Kong H, Jiang Y, Gao Y, Deng G, et al. H5N1 Hybrid Viruses Bearing 2009/H1N1 Virus Genes Transmit in Guinea Pigs by Respiratory Droplet. Science. 2013; 340(6139):1459–63. doi: 10.1126/science.1229455 PMID: 23641061.

48. Stevens J, Blixt O, Chen LM, Donis RO, Paulson JC, Wilson IA. Recent avian H5N1 viruses exhibit increased propensity for acquiring human receptor specificity. J Mol Biol. 2008; 381(5):1382–94. doi: 10.1016/j.jmb.2008.04.016 PMID: 18672252; PubMed Central PMCID: PMC2519951.

49. Chen W, Sun S, Li Z. Two glycosylation sites in H5N1 influenza virus hemagglutinin that affect binding preference by computer-based analysis. PLoS One. 2012; 7(6):e38794. doi: 10.1371/journal.pone.0038794 PMID: 22719948; PubMed Central PMCID: PMC3375263.

50. Kaverin NV, Matrosovich MN, Gambaryan AS, Rudneva IA, Shilov AA, Varich NL, et al. Intergenic HA-NA interactions in influenza A virus: postreassortment substitutions of charged amino acid in the hemagglutinin of different subtypes. Virus Res. 2000; 66(2):123–9. PMID: 10725545.

51. Zaraket H, Bridges OA, Russell CJ. The pH of activation of the hemagglutinin protein regulates H5N1 influenza virus replication and pathogenesis in mice. J Virol. 2013; 87(9):4826–34. doi: 10.1128/JVI.03110-12 PMID: 23449784; PubMed Central PMCID: PMC3624295.

52. Colman PM. Influenza virus neuraminidase: structure, antibodies, and inhibitors. Protein Sci. 1994; 3 (10):1687–96. doi: 10.1002/pro.5560031007 PMID: 7849585; PubMed Central PMCID: PMC2142611.

53. Matrosovich MN, Matrosovich TY, Gray T, Roberts NA, Klenk HD. Neuraminidase is important for the initiation of influenza virus infection in human airway epithelium. J Virol. 2004; 78(22):12665–7. doi: 10.1128/JVI.78.22.12665–12667.2004 PMID: 15507653; PubMed Central PMCID: PMC525087.

54. Palese P, Tobita K, Ueda M, Compans RW. Characterization of temperature sensitive influenza virus mutants defective in neuraminidase. Virology. 1974; 61(2):397–410. PMID: 4472498.

55. Ohuchi M, Asaoka N, Sakai T, Ohuchi R. Roles of neuraminidase in the initial stage of influenza virus infection. Microbes and infection / Institut Pasteur. 2006; 8(5):1287–93. doi: 10.1016/j.micinf.2005.12.008 PMID: 16682242.

56. Su B, Wurtzer S, Rameix-Welti MA, Dwyer D, van der Werf S, Naffakh N, et al. Enhancement of the influenza A hemagglutinin (HA)-mediated cell-cell fusion and virus entry by the viral neuraminidase (NA). PLoS One. 2009; 4(12):e8495. doi: 10.1371/journal.pone.0008495 PMID: 20041119; PubMed Central PMCID: PMC2795206.

57. Els MC, Air GM, Murti KG, Webster RG, Laver WG. An 18-amino acid deletion in an influenza neuraminidase. Virology. 1985; 142(2):241–7. PMID: 4060573.

58. Zimmermann P, Manz B, Haller O, Schwemmle M, Kochs G. The viral nucleoprotein determines Mx sensitivity of influenza A viruses. J Virol. 2011; 85(16):8133–40. doi: 10.1128/JVI.00712-11 PMID: 21680506; PubMed Central PMCID: PMC3147989.

59. Dittmann J, Stertz S, Grimm D, Steel J, Garcia-Sastre A, Haller O, et al. Influenza A virus strains differ in sensitivity to the antiviral action of Mx-GTPase. J Virol. 2008; 82(7):3624–31. doi: 10.1128/JVI.01753-07 PMID: 18199636; PubMed Central PMCID: PMC2268464.

60. Chen L, Zanker D, Xiao K, Wu C, Zou Q, Chen W. Immunodominant CD4+ T-cell responses to influenza A virus in healthy individuals focus on matrix 1 and nucleoprotein. J Virol. 2014; 88(20):11760–73. doi: 10.1128/JVI.01631-14 PMID: 25078703; PubMed Central PMCID: PMC4178733.

61. Bourret V, Croville G, Mariette J, Klopp C, Bouchez O, Tiley L, et al. Whole-genome, deep pyrosequencing analysis of a duck influenza A virus evolution in swine cells. Infect Genet Evol. 2013; 18:31–41. doi: 10.1016/j.meegid.2013.04.034 PMID: 23660486.

62. Li Z, Watanabe T, Hatta M, Watanabe S, Nanbo A, Ozawa M, et al. Mutational analysis of conserved amino acids in the influenza A virus nucleoprotein. J Virol. 2009; 83(9):4153–62. doi: 10.1128/JVI.02642-08 PMID: 19225007; PubMed Central PMCID: PMC2668439.

63. Kao RY, Yang D, Lau LS, Tsui WH, Hu L, Dai J, et al. Identification of influenza A nucleoprotein as an antiviral target. Nat Biotechnol. 2010; 28(6):600–5. doi: 10.1038/nbt.1638 PMID: 20512121.

64. Ilyushina NA, Khalenkov AM, Seiler JP, Forrest HL, Bovin NV, Marjuki H, et al. Adaptation of pandemic H1N1 influenza viruses in mice. J Virol. 2010; 84(17):8607–16. doi: 10.1128/JVI.00159-10 PMID: 20592084; PubMed Central PMCID: PMC2918990.

65. Manz B, Dornfeld D, Gotz V, Zell R, Zimmermann P, Haller O, et al. Pandemic influenza A viruses escape from restriction by human MxA through adaptive mutations in the nucleoprotein. PLoS Pathog. 2013; 9(3):e1003279. doi: 10.1371/journal.ppat.1003279 PMID: 23555271; PubMed Central PMCID: PMC3610643.

66. Cheung PP, Watson SJ, Choy KT, Fun Sia S, Wong DD, Poon LL, et al. Generation and characterization of influenza A viruses with altered polymerase fidelity. Nature communications. 2014; 5:4794. doi: 10.1038/ncomms5794 PMID: 25183443; PubMed Central PMCID: PMC4155405.

67. Driskell EA, Pickens JA, Humberd-Smith J, Gordy JT, Bradley KC, Steinhauer DA, et al. Low pathogenic avian influenza isolates from wild birds replicate and transmit via contact in ferrets without prior adaptation. PLoS One. 2012; 7(6):e38067. doi: 10.1371/journal.pone.0038067 PMID: 22675507; PubMed Central PMCID: PMC3365887.

68. Wu HS, Yang JR, Liu MT, Yang CH, Cheng MC, Chang FY. Influenza A(H5N2) virus antibodies in humans after contact with infected poultry, Taiwan, 2012. Emerg Infect Dis. 2014; 20(5):857–60. doi: 10.3201/eid2005.131393 PMID: 24750594; PubMed Central PMCID: PMC4012807.

69. Wu H, Peng X, Xu L, Jin C, Cheng L, Lu X, et al. Novel reassortant influenza A(H5N8) viruses in domestic ducks, eastern China. Emerg Infect Dis. 2014; 20(8):1315–8. doi: 10.3201/eid2008.140339 PMID: 25075453; PubMed Central PMCID: PMC4111196.

70. Jeong J, Kang HM, Lee EK, Song BM, Kwon YK, Kim HR, et al. Highly pathogenic avian influenza virus (H5N8) in domestic poultry and its relationship with migratory birds in South Korea during 2014. Vet Microbiol. 2014; 173(3–4):249–57. doi: 10.1016/j.vetmic.2014.08.002 PMID: 25192767.

71. Varble A, Albrecht RA, Backes S, Crumiller M, Bouvier NM, Sachs D, et al. Influenza a virus transmission bottlenecks are defined by infection route and recipient host. Cell host & microbe. 2014; 16(5):691–700. doi: 10.1016/j.chom.2014.09.020 PMID: 25456074; PubMed Central PMCID: PMC4272616.

72. Chen H, Yuan H, Gao R, Zhang J, Wang D, Xiong Y, et al. Clinical and epidemiological characteristics of a fatal case of avian influenza A H10N8 virus infection: a descriptive study. Lancet. 2014; 383 (9918):714–21. doi: 10.1016/S0140-6736(14)60111-2 PMID: 24507376.

73. Chan RW, Chan MC, Nicholls JM, Malik Peiris JS. Use of ex vivo and in vitro cultures of the human respiratory tract to study the tropism and host responses of highly pathogenic avian influenza A (H5N1) and other influenza viruses. Virus Res. 2013; 178(1):133–45. doi: 10.1016/j.virusres.2013.03.003 PMID: 23684848; PubMed Central PMCID: PMC3805758.

74. Mok CK, Chang SC, Chen GW, Lo YL, Chen SJ, Wu HS, et al. Pyrosequencing reveals an oseltamivir-resistant marker in the quasispecies of avian influenza A (H7N9) virus. J Microbiol Immunol Infect. 2013. doi: 10.1016/j.jmii.2013.09.010 PMID: 24388586.

75. Marjuki H, Mishin VP, Chesnokov AP, Jones J, De La Cruz JA, Sleeman K, et al. Characterization of drug-resistant influenza A(H7N9) variants isolated from an oseltamivir-treated patient in Taiwan. J Infect Dis. 2015; 211(2):249–57. doi: 10.1093/infdis/jiu447 PMID: 25124927.